Medicinal Chemistry Research (2021) 30:1294–1308
https://doi.org/10.1007/s00044-021-02740-7

MEDICINAL CHEMISTRY RESEARCH

ORIGINAL RESEARCH

Discovery of *N*-phenyl-1-(phenylsulfonamido)cyclopropane-1-carboxamide analogs as NLRP3 inflammasome inhibitors

Wanwan Li[1] · Zhongqiang Cao[1] · Junjie Cheng[1] · Feiyu Chen[1] · Shuai Li[1] · Yiwei Huang[1] · Long Tai Zheng[1] · Na Ye[1]

Received: 26 March 2021 / Accepted: 3 May 2021 / Published online: 16 May 2021

Abstract

Two series of novel NLRP3 inflammasome inhibitors are designed, synthesized, and evaluated in an effort to develop diversified analogs based on the *N*-(phenylcarbamoyl)benzenesulfonamide scaffold. SAR studies reveal that the sulfonylurea linker can tolerate chemical modifications with either simply changing over the position of carbonyl and sulfonyl group or structurally flexibly inserting a cyclopropyl group, leading to identification of several more potent and diversified NLRP3 antagonists (e.g., **9**) with low nanomolar inhibitory activities. Further studies indicate that these two series of compounds with low cytotoxicity exhibited weak effects on the generation of NO and TNF-a. The findings may serve as good starting points for the development of more potent NLRP3 inflammasome inhibitors as valuable pharmacological probes or potential drug candidates.

Keywords Microglia cells · Lipopolysaccharide (LPS) · NLRP3 inflammasome · Nigericin · IL-1β · Inhibitors

Introduction

Microglia-mediated neuroinflammation actively implicated in the progression of neurodegenerative diseases such as Parkinson's disease, Alzheimer's disease, Multiple sclerosis, and HIV-associated dementia [1]. As the resident macrophage cells in brain, microglia continually monitor surrounding tissue to maintain homeostasis of brain in physiological conditions, but in neurodegenerative or inflammatory conditions, it is often activated and can produce number of proinflammatory factors including IL-1β as well as neurotoxic mediators such as nitric oxide (NO) and reactive oxygen species (ROS) [2]. As a proinflammatory cytokine, IL-1β is produced by activated microglia cells to trigger inflammatory responses in brain [3]. Unlike tumor necrosis factor α (TNF-α) and IL-6, secretion of IL-1β needs activation of NLR family pyrin domain containing 3 (NLRP3) mediated inflammasome besides activation of nuclear factor-kappa B (NF-κB) signaling pathway [4]. Once secreted, IL-1β can stimulate the surrounding microglia or astrocytes to produce another proinflammatory factors such as TNF-α, iNOS, COX-2, and IL-6, which contributed to neuronal cell death and injuries [3]. Therefore, inhibition of NLRP3 inflammasome activation would be an effective therapeutic strategy for neuroinflamamtory diseases.

NLRP3 inflammasome as the most well-known inflammasome is a cytosolic multiprotein signaling complex that mediates the secretion of potent inflammatory mediators [5–7], and is associated with the pathogenesis of many common neurodegenerative diseases [8–22] including Parkinson's disease, Alzheimer disease, and ischemic stroke. Activation of the NLRP3 inflammasome is known to be controlled by activation of two step signal, priming step (signal 1) and activating step (signal 2). The signal 1 is induced by activation of transcriptional factor NF-κB, resulting in upregulation of NLPR3 and pro-IL-1β. The signal 2 is triggered by various intra- or extra-stimuli such as extracellular ATP, nigericin, viral RNA, lysosomal

These authors contributed equally: Wanwan Li, Zhongqiang Cao

Supplementary information The online version contains supplementary material available at https://doi.org/10.1007/s00044-021-02740-7.

✉ Long Tai Zheng
zhenglongtai@suda.edu.cn

✉ Na Ye
yena@suda.edu.cn

[1] Jiangsu Key Laboratory of Neuropsychiatric Diseases and College of Pharmaceutical Sciences, Soochow University, Suzhou, Jiangsu 215123, China

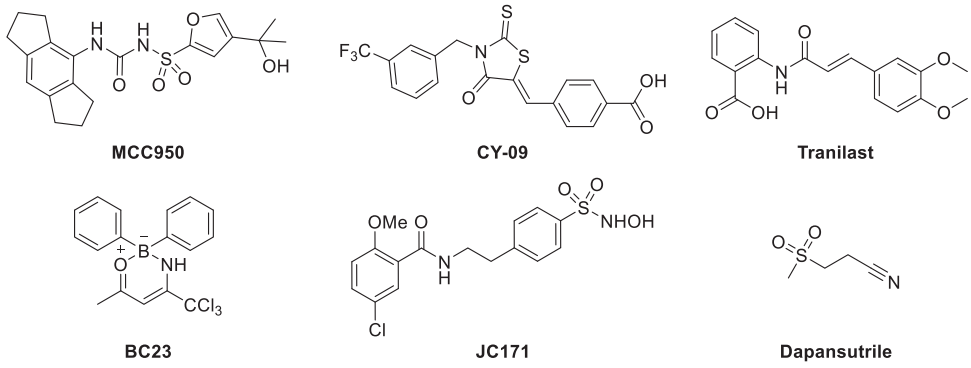

Fig. 1 Small molecule inhibitors targeting the NLRP3 inflammasome pathway

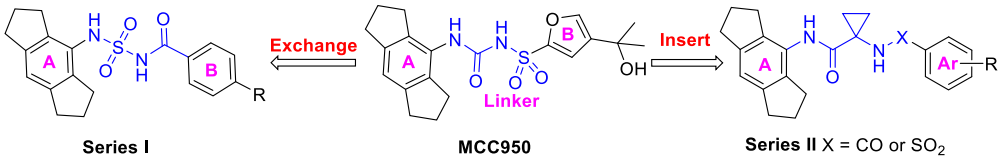

Fig. 2 Drug design strategy for the current work

damage, aggregated amyloid beta, ROS production, or mitochondrial metabolism following signal 1 activation. Upon response to those signaling events, NLRP3 initiates recruitment of the adapter apoptosis-associated speck-like protein containing a C-terminal caspase recruitment domain (ASC) and caspase-1, resulting in production of mature IL-1β and IL-18 [6, 7].

Many small molecules have been developed as direct or indirect NLRP3 inflammasome inhibitors (e.g., Fig. 1), but there are still no NLRP3 antagonists approved for therapeutic use [6, 7, 23–25]. One of the most well-characterized NLRP3 inflammasome inhibitors is the sulfonylurea analog—MCC950 (also called CRID3 and CP-446,773), which was initially identified by Perregaux et al. as the most potent inhibitor of IL-1β release (IC_{50} = 8.1 nM in bone-marrow-derived macrophage (BMDM) cells) [26]. MCC950 as a useful tool compound displays efficacy in a wide range of animal disease models [7] including Alzheimer's disease [27], Parkinson's disease [19], multiple sclerosis [28], myocardial infarction [29], atherosclerosis [30], stroke [31], asthma and allergic airway inflammation [32], and cryopyrin-associated periodic syndromes [16]. Although MCC950 was tested in phase II clinical trials for rheumatoid arthritis, it was not progressed further due to its liver toxicity [7]. The combination of its metabolically reactive furan moiety and sulfonylurea linker, which may generate the cis-enedione and isocyanate in vivo respectively, and subsequent conjugate with biological macromolecules, might underlie the observed toxicity [33, 34]. In 2016, Robertson group provided first insight into the SAR of the hexahydroindacene moiety of MCC950, and found that this tricyclic moiety is largely indispensable for good bioactivity in human monocyte-derived macrophages [35, 36]. Later, three different research groups reported that MCC950 can tolerate its furan moiety to be modified with phenyl rings [37–39]. Currently, its sulfonylurea linker was reported to be replaced with *N*-cyanosulfoximineurea [38] and ester substituted linker [40] resulting in nanomolar activity in THP1 cells and human peripheral blood mononuclear cells, respectively.

As depicted in Fig. 2, we designed and synthesized two newly diversified series as NLPR3 inflammasome inhibitors by chemical modifications of the sulfonylurea linker on the *N*-(phenylcarbamoyl)benzenesulfonamide scaffold of MCC950 and replacement of its furan ring B with phenyl rings. Series I was designed by changing over the position of carbonyl and sulfonyl group in the sulfonylurea linker, while series II was designed to make the compact linker flexible by inserting a cyclopropyl group in the middle in view of versatile cyclopropyl fragments frequently appeared in preclinical/clinical drug molecules [41]. Herein, we report that such structural modifications on the *N*-(phenylcarbamoyl)benzenesulfonamide scaffold have resulted in the discovery of several structural diverse NLRP3 inflammasome inhibitors such as **9** with low nanomolar inhibitory activities.

Results and discussion

Chemistry

The synthesis of new derivatives based on *N*-(phenylcarbamoyl)benzenesulfonamide scaffold with chemical optimizations on the linker and phenyl ring B is outlined in Schemes 1 and 2. 1,2,3,5,6,7-hexahydro-*s*-indacen-4-amine **1**,

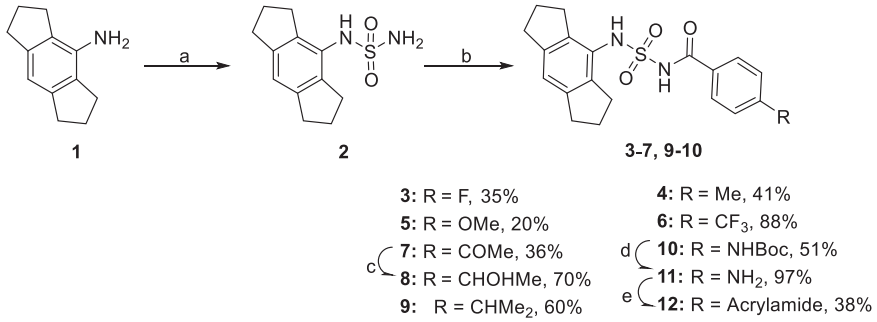

Scheme 1 The synthesis of series I compounds. Reagents and conditions: (a) (i) $ClSO_2NCO$, Et_3N, *t*-BuOH, CH_2Cl_2, 0 °C, rt, 2 h; (ii) conc. HCl:EtOAc = 1:2, rt, 1 h; 50% for two steps. (b) RCOOH, CDI, DBU, THF, 70 °C, 24 h, 20–97%. (c) $NaBH_4$, EtOH, 80 °C, 12 h, 70%. (d) conc. HCl:EtOAc = 1:2, rt, 2 h, 97%. (e) Acryloyl chloride, DIPEA, DMF, rt, 3 h, 38%

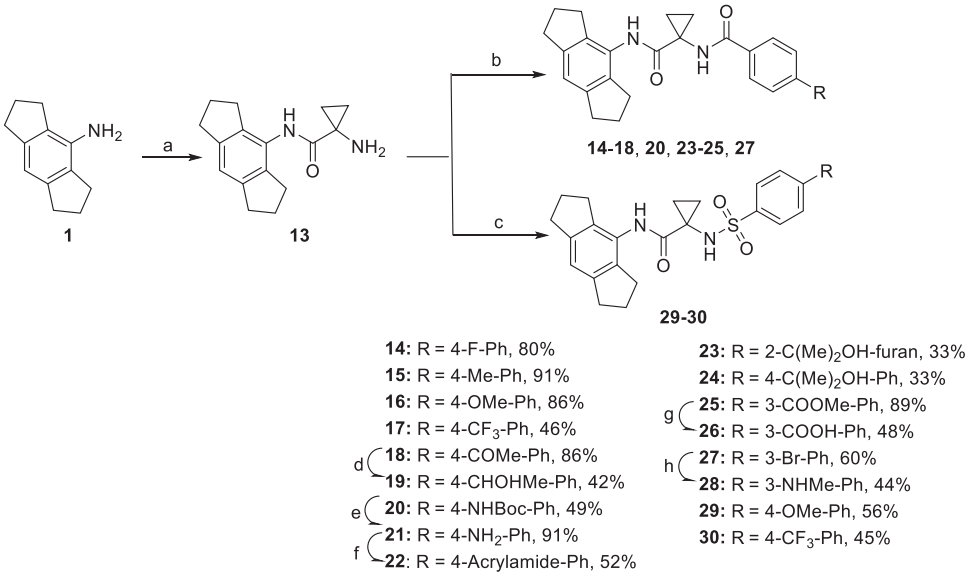

Scheme 2 The synthesis of series II compounds. Reagents and conditions: (a) (i) EDCI, HOBt, Et_3N, DCM, rt, 24 h; (ii) conc. HCl: EtOAc = 1: 2, rt, 1 h; 59% for two steps. (b) RCOOH, EDCI, HOBt, Et_3N, DCM, rt, 24 h, 27–91%. (c) RSO_2Cl, pydine, DCM, rt, 16 h, 45–56%. (d) $NaBH_4$, EtOH, 80 °C, 12 h, 42%. (e) conc. HCl: EtOAc = 1: 2, rt, 2 h, 91%. (f) Acryloyl chloride, DIPEA, DMF, rt, 3 h, 52%. (g) LiOH, THF, H_2O, rt, 2 h, 48%. (h) Cu, $MeNH_2$, 100 °C, 22 h, 43%

prepared from commercially available 2,3-dihydro-1*H*-indene by following a literature procedure [42], was used as the key intermediate. Condensation of **1** with chlorosulfonyl isocyanate and 1-((*tert*-butoxycarbonyl)amino)cyclopropane-1-carboxylic acid, and then deprotection, provide key intermediates **2** and **13** in 50% and 59% overall yield, respectively. As outlined in Scheme 1, series I compounds **3–7** and **9–10** were prepared by condensation of **2** with the commercially available acids under the treatment of CDI and DBU in 20–97% yields. Similarly, amidation or sulfonamidation of amide **13** with the commercially available corresponding acids or sulfonyl chloride yielded series II compounds **14–18**, **20**, **23–25**, **27**, and **29–30** in 33–91% yields (Scheme 2). Subsequently, reduction of alcohols **7** and **18** with $NaBH_4$ at reflux yield **8** and **19** in 70% and 42%, respectively. Hydrolysis of esters **25** with LiOH yielded corresponding acids **26** in 48% yield. Deprotection of Boc group in **10** and **20** obtained amines **11** and **21** in 97% and 91% yield, followed by acylation with acryloyl chloride led to **12** and **22** in 38% and 52% yield, respectively. The synthesized final compounds were analyzed by ^1H NMR, ^{13}C NMR, and high-resolution mass spectra (HRMS).

Cytotoxicity of the target compounds 3–12 and 14–30

Since cytotoxicity may affect the inhibitory effects of compounds on cytokines production in microglia cells, we firstly evaluated the effect of compounds on cell viability by 3-(4,5-dimethylthiazol-2-yl)-2,5-diphenyltetrazolium-bromide (MTT) assay in BV-2 microglia cells. As shown in Fig. 3, most compounds at concentrations of 20 μM showed no obvious cytotoxicity in BV-2 microglia cells, with the fact that the relative cell viability is higher than 95% except for that of compound **10** (88.34 ± 1.68%). Thus, 20-μM concentration was chosen for subsequent screening experiments.

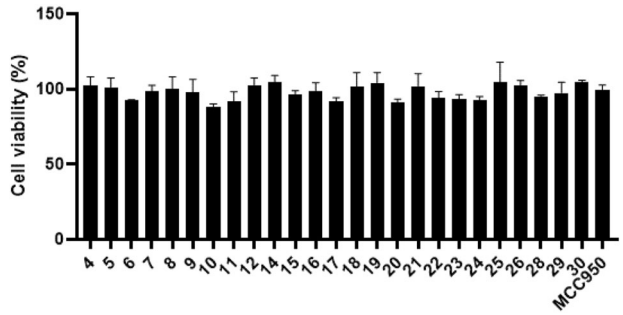

Fig. 3 The effect of compounds on the viability of BV-2 microglia cells

Table 1 The inhibitory effect of series I compounds on the production of IL-1β in LPS/nigericin-stimulated primary microglia cells

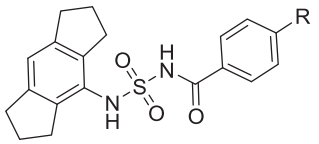

No.	R	Inhibition rate of IL-1β (%)[a]	
		10 μM	20 μM
3	F	50.90 ± 0.63	55.64 ± 0.63
4	Me	56.70 ± 2.92	65.32 ± 1.46
5	OMe	59.88 ± 4.54	66.67 ± 1.51
6	CF_3	–	48.38 ± 0
7	Ac	41.71 ± 3.02	55.13 ± 1.51
8	CHOHMe	57.75 ± 1.51	64.10 ± 3.02
9	i-Pr	60.95 ± 3.02	69.23 ± 3.02
10	NHBoc	–	48.38 ± 0
11	NH_2	–	45.76 ± 7.19
12	Acrylamide	54.03 ± 2.53	62.82 ± 1.89
[b]**MCC950**		73.20 ± 2.92	87.63 ± 2.92

[a]The primary microglia cells were primed with LPS (100 ng/ml) for 3 h (10 and 20 μM) 30 min before stimulation of nigericin (25 μM). After treatment of nigericin for 30 min, the amounts of IL-1β in cell culture supernatants were measured by ELISA. MCC950 served as positive control, while DMSO served as vehicle control. All data were expressed as mean ± S.D ($n = 3$) and representative of three independent experiments

[b]The concentrations of MCC950 were 100 nM and 1 μM. "–" indicates that the activity is not tested

In vitro evaluation on IL-1β production inhibition

The NLRP3 inhibition of each compound was first tested at a concentration of 20 μM by measuring IL-1β secretion from primary microglia cells, the innate immune cells in the central nervous system (CNS). Lipopolysaccharide (LPS)-primed primary microglia cells were pretreated with the test compounds, and then stimulated with inflammasome activator nigericin. The levels of IL-1β in cell culture media were measured by enzyme-linked immunosorbent assay (ELISA) (Tables 1 and 2). Compounds with inhibition at 20 μM higher than 50% were further evaluated for the second round of screening at 10 μM. And the inhibition of reference compound MCC950 is 87.6% and 73.2% at 1 μM and 100 nM, respectively.

Table 2 The inhibitory effect of series II compounds on the production of IL-1β in LPS/nigericin-stimulated primary microglia cells

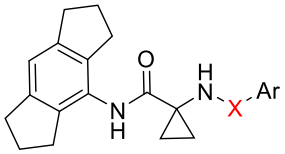

No.	X	Ar	Inhibition rate of IL-1β (%)[a]	
			10 μM	20 μM
14	CO	4-F-Ph	38.50 ± 1.51	50.80 ± 3.02
15	CO	4-Me-Ph	47.42 ± 4.37	67.73 ± 2.92
16	CO	4-OMe-Ph	49.56 ± 1.26	64.10 ± 2.53
17	CO	4-CF_3-Ph	51.55 ± 4.37	67.74 ± 2.92
18	CO	4-COMe-Ph	56.68 ± 3.02	67.95 ± 1.51
19	CO	4-CHOHMe-Ph	57.75 ± 4.54	65.39 ± 1.51
20	CO	4-NHBoc-Ph	51.55 ± 4.37	63.56 ± 2.92
21	CO	4-NH_2-Ph	59.88 ± 4.54	66.67 ± 1.51
22	CO	4-Acrylamide-Ph	–	45.76 ± 0
23	CO	2-C(Me)$_2$OH-Furan	–	45.76 ± 4.36
24	CO	4-C(Me)$_2$OH-Ph	–	48.30 ± 0
25	CO	3-COOMe-Ph	68.31 ± 2.53	75.64 ± 0.63
26	CO	3-COOH-Ph	50.45 ± 2.53	64.10 ± 1.26
28	CO	3-NHMe	38.50 ± 4.54	50.84 ± 3.02
29	SO_2	4-OMe-Ph	70.10 ± 1.26	70.51 ± 1.26
30	SO_2	4-CF_3-Ph	65.63 ± 2.53	70.51 ± 1.26
[b]**MCC950**			73.20 ± 2.92	87.63 ± 2.92

[a]The primary microglia cells were primed with LPS (100 ng/ml) for 3 h and then the cells were pretreated with compounds (10 and 20 μM) for 30 min before stimulation of nigericin (25 μM). After treatment of nigericin for 30 min, the amounts of IL-1β in cell culture supernatants were measured by ELISA. MCC950 served as positive control, while DMSO served as vehicle control. All data were expressed as mean ± S.D ($n = 3$) and are representative of three independent experiments

[b]The concentrations of MCC950 were 100 nM and 1 μM. "–" indicates that the activity is not tested

As shown in Table 1, we initially investigated the electronic effect of substitutions on the phenyl ring B in series I. Introduction with electro-withdrawing groups as in compounds **3**, **6**, and **7** generally led to a slight loss of activity compared to that of compounds **4**, **5**, and **8**–**9** with electro-donating groups. The most potent compound **9** with a bulky isopropyl group displays an inhibitory activity of 61% at 10 μM. Unexpectedly, compounds with bulky group, hydrogen bond donor or Michael receptor (as in compound **10**–**12**), all decrease potency, suggesting that the substitutions on the phenyl ring B play an important role in NLRP3 inhibition.

In series II as shown in Table 2, a flexible linker by inserting a cyclopropyl group, results in a dramatically different SAR result from series I. Their activities are independent on the electronic and steric effect of substitutions on the 4-position of phenyl ring B (as in compounds **14**–**18**). The compounds with electro-withdrawing groups such as F (e.g., **14** vs. **3**) reduce potency, while compounds with CF_3, and Ac group enhance potency (e.g., **17** vs. **6**; **18** vs. **7**). In addition, the compounds with electro-donating groups such as Me and OMe (e.g., **15** vs. **4**; **16** vs. **5**) reduce potency, while compounds with NHBoc and NH_2 group enhance potency (e.g., **20** vs. **10**; **21** vs. **11**). These results suggest that the 4-position of the phenyl ring B of series II can tolerate chemical modifications with either electron-withdrawing or -donating groups. Compound **22** with a covalent warhead, which may interact with NLRP3 proteins, is also inactive. Moreover, introduction of the same furan B ring as MCC950 (as in compound **23**) lost potency. Alternatively, introduction of the phenyl ring B with the same substitution, 2-hydroxypropan-2-yl group, still lost activity. Surprisingly, switching the substitution to 3-position (as in compounds **25**–**38**) leads to the discovery of ester **25** as the most potent compound in series II, with an inhibitory activity of 68.3% at 10 μM. To our great delight, the potency also boosts by replacement an amide with a sulfamide linker in compounds **16**–**17**, leading to compounds **29**–**30** with an inhibitory activity of 65–70% at 10 μM (Fig. 3).

All these above findings suggest that the sulfonylurea linker on the *N*-(phenylcarbamoyl)benzenesulfonamide scaffold by replacing furan ring B of MCC950 with phenyl rings can tolerate chemical modifications with either simply changing over the position of carbonyl and sulfonyl group or inserting a cyclopropyl group to be flexible.

Compounds 9, 25, 29–30 inhibit the production of IL-1β in a concentration-dependent manner

We selected compounds with inhibition of the production of IL-1β at 10 μM higher than 50% to further determine their half-maximal inhibitory concentration (IC_{50}, Table 3). Calculated partition coefficient (clogP) and topological polar surface area (TPSA) are the fundamental physicochemical properties to evaluate their drug-like properties. All these selected compounds have the acceptable clogP and TPSA values for CNS drug candidates (Table 3). Among these analogs, compound **9** in series I and compounds **25** and **29**–**30** in series II remarkably inhibited the production of IL-1β in a concentration-dependent manner in primary microglia cells, with IC_{50} values of 2.05–4.48 μM (Fig. 4). Compounds **9**, **25**, and **29**–**30** were also evaluated their inhibition on the production of IL-1β in the BMDMs stimulated by LPS/ATP. Surprisingly, only compound **9** concentration dependently inhibited the production of IL-1β with an IC_{50} value of 30.62 ± 1.49 nM (Fig. 5A, B). Compound **9** is slightly more lipophilic than compounds **25**, **29**, and **30**, and its TPSA value is slightly lower than the other three compounds (Table 3), indicating that compound **9** may have better membrane permeability [43]. Distinct IC_{50} value of primary microglia cells and BMDMs may be attributed to distinct expression of drug-metabolism-related genes or different cell membrane permeability between these two cell types.

We also evaluated the effect of compound **9** on TNF-a production in LPS/ATP-treated BMDM. As shown in Fig. 5C, D, compound **9** did not impaired TNF-a secretion, suggesting that the inhibition of IL-1β production was NLRP3-specific.

Table 3 The IC_{50} values of potent compounds in inhibiting the production of IL-1β in primary microglia cells

No	cLogP[a]	TPSA[b]	IL-1β IC_{50} (μM)[c]
4	3.07	75.27	6.36 ± 0.80
5	3.09	84.50	6.64 ± 0.82
8	2.73	95.50	8.00 ± 0.90
9	4.03	75.27	4.48 ± 0.65
17	4.25	58.20	8.60 ± 0.93
18	3.26	75.27	6.07 ± 0.78
19	3.07	78.42	7.93 ± 0.90
20	3.91	96.53	7.53 ± 0.88
21	2.75	84.22	7.74 ± 0.89
25	3.29	84.50	2.05 ± 0.31
29	2.60	84.50	2.12 ± 0.33
30	3.54	75.27	2.78 ± 0.44
MCC950	2.54	108.64	–

[a]http://146.107.217.178/lab/alogps/start.html

[b]https://www.molinspiration.com/cgi-bin/properties#

[c]The primary microglia cells were primed with LPS (100 ng/ml) for 3 h and then the cells were pretreated with compounds for 30 min before stimulation of nigericin (25 μM). After treatment of nigericin for 30 min, the amounts of IL-1β in cell culture supernatants were measured by ELISA. All data were expressed as mean ± S.D ($n = 3$) and are representative of three independent experiments

In vitro evaluation of NO inhibition

LPS induces expression of pro-IL-1β and NLRP3 in microglia cells via activation of NF-κB signaling pathway [44, 45]. NO is an important neuroinflammatory factor that is secreted by LPS-activated microglia cells and contributes to neuronal damage and apoptosis, and its production is independent of NLRP3 inflammasome activation, but dependent on activation of NF-κB signaling pathway [46–49]. Therefore, NO production may partly reflect the levels

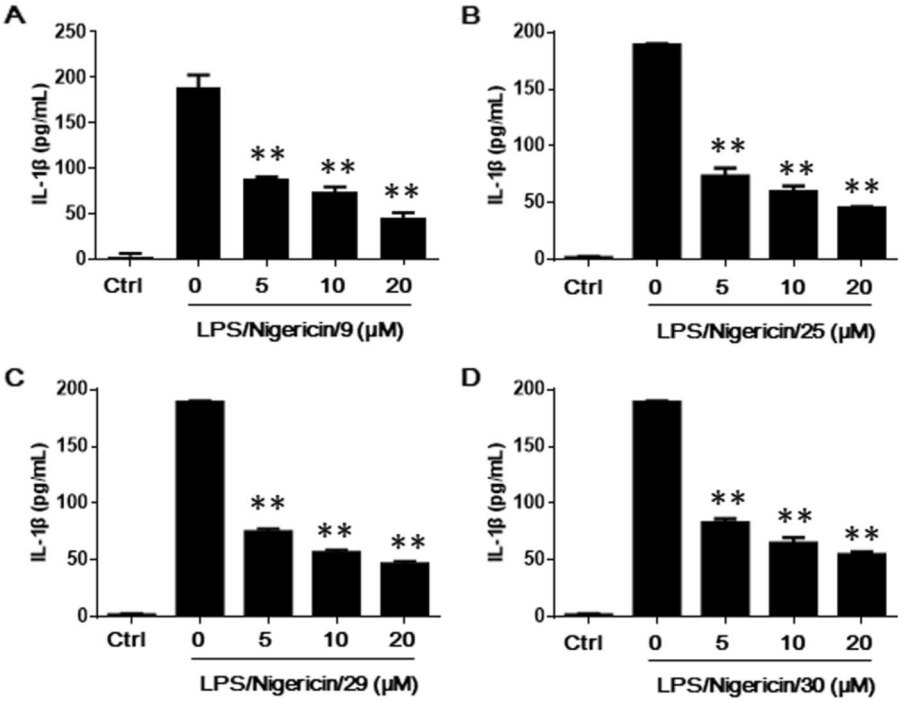

Fig. 4 Compounds **9**, **25**, **29**, and **30** block NLRP3 inflammasome activation in primary microglia cells. **A–D** The primary microglia cells were primed with LPS (100 ng/ml) for 3 h and then the cells were pretreated with indicated concentration of compounds for 30 min before stimulation of nigericin (25 μM). After treatment of nigericin for 30 min, the amounts of IL-1β in cell culture supernatants were measured by ELISA. All data were expressed as mean ± S.D ($n = 3$) and are representative of three independent experiments. $^{**}P < 0.01$ and $^{***}P < 0.001$ compared to LPS/nigericin-treated alone group

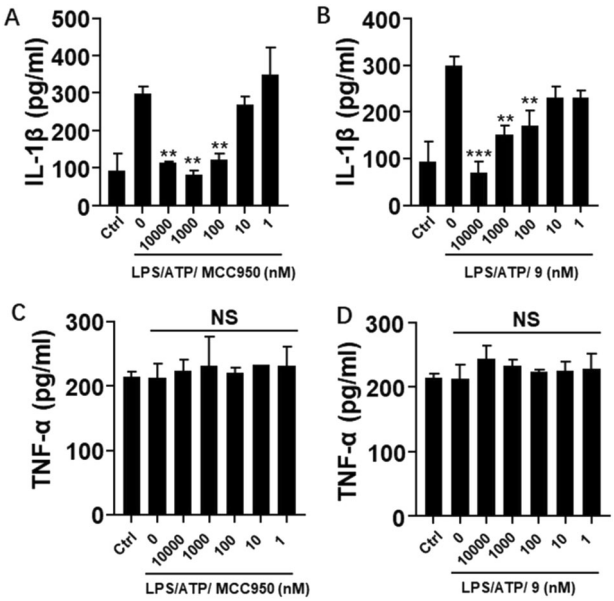

Fig. 5 Compounds **9** and **MCC950** suppress ATP-induced NLRP3 inflammasome activation in BMDMs. The BMDMs were primed with LPS (100 ng/ml) for 3 h and then the cells were pretreated with indicated concentration of compounds for 30 min before stimulation of ATP (3 mM). After treatment of nigericin for 30 min, the amounts of IL-1β (**A, B**) or TNF-α (**C, D**) in cell culture supernatants were measured by a specific ELISA kit, respectively. All data were expressed as mean ± S.D ($n = 3$) and are representative of three independent experiments. $^{**}P < 0.01$ and $^{***}P < 0.001$ compared to LPS/ATP alone treated group

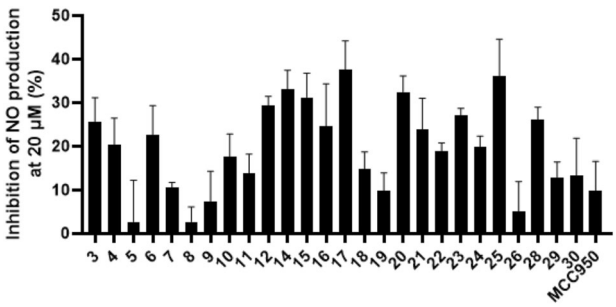

Fig. 6 The effects of compounds on NO production in LPS-activated BV-2 microglia cells. BV-2 microglia cells were pretreated with compounds (20 μM) for 30 min and then incubated with LPS for 24 h. The production of NO in cell culture supernatant was measured by Griess agents. The formula to calculate the percent of inhibition is following: % inhibition = [1 − (NO amounts of compound treatment in the presence of LPS − NO amounts of compound alone treatment)/(NO amounts of LPS alone treatment − NO amounts of control)] × 100. Data shown as mean ± S.D. ($n = 3$)

of pro-IL-1β and NLRP3 in LPS-activated microglia cells. We thus further confirmed whether our compounds inhibited the activation of NF-κB signaling pathway by evaluating their inhibitory effects on LPS-induced NO generation. As shown in Fig. 6, all these NLRP3 inhibitors exhibited weak inhibitory activity on NO production by <40% inhibition at 20 μM, indicating that inhibition of IL-1β production was independent of signal 1.

Conclusions

Two series of novel NLRP3 inflammasome inhibitors based on the *N*-(phenylcarbamoyl)benzenesulfonamide scaffold by replacing furan ring B of MCC950 with phenyl rings have been designed and synthesized. The SAR results indicate that their sulfonylurea linker can tolerate chemical modifications with either simply changing over the position of carbonyl and sulfonyl group or structurally flexibly inserting a cyclopropyl group. All these modification efforts allow us to further tune MCC950 to achieve more potent and structurally diverse NLRP3 inflammasome inhibitors, e.g., compound **9** with an IC_{50} value of 30.62 nM in BMDMs stimulated by LPS/ATP. Compound **9** may hold promise as a potential drug candidate toward novel therapeutics against human diseases, and serve as a valuable pharmacological probe to elucidate the physiological functions of NLRP3 inflammasome.

Experimental

Chemistry

All commercially available starting materials and solvents were reagent grade, and used without further purification. Reactions were performed under a nitrogen atmosphere in dry glassware with magnetic stirring. Column chromatography was carried out on silica gel (200–300 mesh). All reactions were monitored using thin layer chromatography on silica gel plates. Visualization of the developed chromatograms was performed with detection by UV (254 and 365 nm). ^{1}H NMR spectra were recorded on 400 or 600 MHz (100 or 150 MHz for ^{13}C NMR) agilent NMR spectrometer. ^{1}H and ^{13}C NMR spectra were recorded with TMS as an internal reference. Chemical shifts were expressed in ppm, and *J* values were given in Hz. HRMS were recorded on a GCT PremierTM (CI) Mass Spectrometer or an Agilent 6540 UHD Accurate-Mass Q-TOF LC/MS.

N-(1,2,3,5,6,7-hexahydro-s-indacen-4-yl) sulfamoylcarbamate (2)

To a stirred solution of chlorosulfonyl isocyanate (0.20 ml, 1.75 mmol) in anhydrous dichloromethane (3 mL) at 0 °C was added *t*-butanol (0.16 mL, 1.75 mmol) in the same solvent. After a period of 30 min, the resulting solution and triethylamine (0.25 mL, 1.75 mmol) were slowly added into a solution of **1** (300 mg, 1.75 mmol) in 2 mL of dichloromethane. The reaction did not rise above 5 °C. The resulting reaction solution was allowed to warm up to room temperature for over 2 h. The reaction mixture diluted with 30 mL of dichloromethane, washed with 1-N HCl and water. The organic layer was dried over Na_2SO_4, filtered, and concentrated in vacuum to give the crude product. The residue was purified by column chromatography on silica gel [Petroleum ether (PE)/EtOAc = 3/1].

To remove the Boc protective group, the product from above was dissolved in 6 mL 1:2 (v/v) mix of conc. HCl:EA and let stay at rt for 1 h. After concentrated and neutralized with ammonia, the reaction mixture was extracted with DCM (30 mL × 2). The combined organic layer was washed with brine (30 mL). dried over anhydrous Na_2SO_4, filtered, and concentrated in vacuum to give the crude product. The residue was purified by column chromatography on silica gel (PE/EtOAc = 2/1), giving product **2** as white solid (192 mg, 44%).^{1}H NMR (400 MHz, DMSO-d_6) δ 8.24 (*s*, 1H), 6.96 (*s*, 1H), 6.72 (*s*, 2H), 2.93 (*t*, $J = 7.1$ Hz, 4H), 2.79 (*t*, $J = 7.1$ Hz, 4H), 1.98–1.89 (*m*, 4H).

General procedures 1 (GP1)

A mixture of benzoic acids (1 eq) and CDI (1.1 eq) in THF (2 mL/mmol) was heated at 70 °C for 45 min under a nitrogen atmosphere, cooled down and added **2** (1.1 eq) and DBU (3 eq). The mixture was stirred for 20–24 h. The reaction mixture was diluted with DCM (30 mL), and washed with 1-N HCl and brine (30 mL). The organic layer was dried over anhydrous Na_2SO_4, filtered, and concentrated in vacuum to give the crude product. The residue was purified by column chromatography on silica gel to afford corresponding products.

3-Fluoro-*N*-(*N*-(1,2,3,5,6,7-hexahydro-s-indacen-4-yl) sulfamoyl)benzamide (3)

According to **GP1**, 4-fluorobenzoic acid (21 mg, 0.3 mmol) and **2** (88 mg, 0.35 mmol) were converted to the desired product **3** (19 mg, 17%) as a white solid. ^{1}H NMR (400 MHz, DMSO-d_6) δ 11.95 (*s*, 1H), 9.71 (*s*, 1H), 7.97 (*dd*, $J = 8.2$, 5.6 Hz, 2H), 7.34 (*t*, $J = 8.7$ Hz, 2H), 7.00 (*s*, 1H), 2.78 (*m*, 8H), 1.92–1.81 (*m*, 4H). ^{13}C NMR (101-MHz, DMSO-d_6) δ 165.2 (*d*, $J_{C\text{-}F} = 251.96$), 165.1, 144.0, 141.3, 131.5 (*d*, $J_{C\text{-}F} = 9.44$), 129.3 (*d*, $J_{C\text{-}F} = 2.83$), 128.4, 120.0, 116.1 (*d*, $J_{C\text{-}F} = 322.11$), 33.0, 30.9, 25.8. HRMS (ESI) calcd for $C_{19}H_{20}FN_2O_3S$ $[M + H]^+$: 375.1179, found 375.1176.

N-(*N*-(1,2,3,5,6,7-hexahydro-s-indacen-4-yl)sulfamoyl)-3-methylbenzamide (4)

According to **GP1**, 4-methylbenzoic acid (20 mg, 0.3 mmol) and **2** (88 mg, 0.35 mmol) were converted to the desired product **4** (46 mg, 41%) as a white solid. ^{1}H NMR (400 MHz, DMSO-d_6) δ 11.82 (*s*, 1H), 9.62 (*s*, 1H), 7.80 (*d*, $J = 7.8$ Hz, 2H), 7.30 (*d*, $J = 7.7$ Hz, 2H), 6.99 (*s*, 1H),

2.83–2.72 (*m*, 8H), 2.36 (*s*, 3H), 1.91–1.81 (*m*, 4H). ^{13}C NMR (101 MHz, DMSO-d_6) δ 166.1, 143.9, 143.5, 141.2, 130.1, 129.6, 128.7, 128.6, 119.9, 33.0, 30.9, 25.8, 21.5. HRMS (ESI) calcd for $C_{20}H_{23}N_2O_3S$ $[M + H]^+$: 371.1429, found 371.1427.

N-(*N*-(1,2,3,5,6,7-hexahydro-s-indacen-4-yl)sulfamoyl)-4-methoxybenzamide (5)

According to **GP1**, 4-methoxybenzoic acid (44 mg, 0.29 mmol) and **2** (80 mg, 0.32 mmol) were converted to the desired product **5** (22 mg, 20%) as a white solid. ^{1}H NMR (400 MHz, DMSO-d_6) δ 11.71 (*s*, 1H), 9.57 (*s*, 1H), 7.89 (*d*, $J = 8.5$ Hz, 2H), 7.03 (*d*, $J = 8.6$ Hz, 2H), 6.99 (*s*, 1H), 3.83 (*s*, 3H), 2.77 (*m*, 8H), 1.90–1.81 (*m*, 4H). ^{13}C NMR (101 MHz, DMSO-d_6) δ 165.5, 163.2, 143.9, 141.3, 130.7, 128.6, 124.8, 119.9, 114.3, 56.0, 33.0, 30.9, 25.8. HRMS (ESI) calcd for $C_{20}H_{23}N_2O_4S$ $[M + H]^+$: 387.1379, found 387.1374.

N-(*N*-(1,2,3,5,6,7-hexahydro-s-indacen-4-yl)sulfamoyl)-3-(trifluoromethyl)benzamide (6)

According to **GP1**, 4-(trifluoromethyl)benzoic acid (34 mg, 0.18 mmol) and **2** (50 mg, 0.20 mmol) were converted to the desired product **6** (42 mg, 55%) as a white solid. ^{1}H NMR (400 MHz, DMSO-d_6) δ 12.20 (*s*, 1H), 9.82 (*s*, 1H), 8.06 (*d*, $J = 7.7$ Hz, 2H), 7.90 (*d*, $J = 7.8$ Hz, 2H), 7.01 (*s*, 1H), 2.77 (*m*, 8H), 1.93–1.81 (*m*, 4H). ^{13}C NMR (151 MHz, DMSO-d_6) δ 165.2, 144.0, 141.2, 136.6, 132.7 (*q*, $J_{C\text{-}F} = 32.1$), 126.1 (*d*, $J_{C\text{-}F} = 3.38$), 126.0 (*q*, $J_{C\text{-}F} = 272.99$), 120.0, 33.0, 30.9, 25.8. HRMS (ESI) calcd for $C_{20}H_{20}F_3N_2O_3S$ $[M + H]^+$: 425.1147, found 425.1141.

Acetyl-*N*-(*N*-(1,2,3,5,6,7-hexahydro-s-indacen-4-yl)sulfamoyl)benzamide (7)

According to **GP1**, 4-acetylbenzoic acid (30 mg, 0.18 mmol) and **2** (50 mg, 0.20 mmol) were converted to the desired product **7** (26 mg, 36%) as a white solid. ^{1}H NMR (400 MHz, DMSO-d_6) δ 12.09 (*s*, 1H), 9.76 (*s*, 1H), 8.03 (*d*, $J = 8.0$ Hz, 2H), 7.97 (*d*, $J = 8.1$ Hz, 2H), 6.98 (*s*, 1H), 2.80–2.69 (*m*, 8H), 2.60 (*s*, 3H), 1.90–1.79 (*m*, 4H). ^{13}C NMR (151 MHz, DMSO-d_6) δ 198.1, 165.5, 144.0, 141.2, 140.1, 136.4, 128.9, 128.7, 128.3, 120.0, 33.0, 30.9, 27.5, 25.8. HRMS (ESI) calcd for $C_{21}H_{23}N_2O_4S$ $[M + H]^+$: 399.1379, found 399.1374.

N-(*N*-(1,2,3,5,6,7-hexahydro-s-indacen-4-yl)sulfamoyl)-4-isopropylbenzamidee (9)

According to **GP1**, 4-isopropylbenzoic acid (40 mg, 0.24 mmol) and compound **2** (67 mg, 0.26 mmol) were converted to the desired product **9** (58 mg, 60%) as a white solid. ^{1}H NMR (400 MHz, DMSO-d_6) δ 11.81 (*s*, 1H), 9.62 (*s*, 1H), 7.82 (*d*, $J = 7.5$ Hz, 2H), 7.37 (*d*, $J = 7.4$ Hz, 2H), 7.00 (*s*, 1H), 3.00–2.92 (*m*, 1H), 2.83–2.73 (*m*, 8H), 1.91–1.80 (*m*, 4H), 1.22 (*s*, 3H), 1.21 (*s*, 3H).^{13}C NMR (151 MHz, DMSO-D_6) δ 166.0, 153.9, 143.9, 141.2, 130.5, 128.8, 128.5, 127.0, 119.9, 33.9, 33.0, 30.9, 25.8, 23.9. HRMS (ESI) calcd for $C_{22}H_{27}N_2O_3S$ $[M + H]^+$: 399.1742, found 399.1738.

tert-Butyl(4-((*N*-(1,2,3,5,6,7-hexahydro-s-indacen-4-yl)sulfamoyl)carbamoyl)phenyl)carbamate (10)

According to **GP1**, 4-((*tert*-butoxycarbonyl)amino) benzoic acid (60 mg, 0.25 mmol) and **2** (71 mg, 0.28 mmol) were converted to the desired product **10** (60 mg, 51%) as a white solid. ^{1}H NMR (400 MHz, DMSO-d_6) δ 11.69 (*s*, 1H), 9.76 (*s*, 1H), 9.57 (*s*, 1H), 7.82 (*d*, $J = 8.3$ Hz, 2H), 7.54 (*d*, $J =$ 8.2 Hz, 2H), 6.99 (*s*, 1H), 2.88–2.67 (*m*, 8H), 1.93–1.81 (*m*, 4H), 1.48 (*s*, 9H). ^{13}C NMR (151 MHz, DMSO-d_6) δ 165.5, 153.0, 144.2, 143.9, 141.3, 129.7, 128.5, 125.8, 119.9, 117.6, 80.2, 33.0, 30.8, 28.5, 25.8. HRMS (ESI) calcd for $C_{24}H_{30}N_3O_5S$ $[M + H]^+$: 472.1906, found 472.1902.

(*N*-(1,2,3,5,6,7-hexahydro-s-indacen-4-yl)sulfamoyl)-4-(1-hydroxyethyl)benzamide (8)

Compound **7** (100 mg, 0.25 mmol) was dissolved in 2-ml ethanol, and sodium borohydride (12 mg, 0.30 mmol) was added to the mixture. The reaction was refluxed at 80 °C for 12 h. The reaction mixture was extracted with DCM (30 mL × 2), and washed with brine. The organic layer was dried over anhydrous Na_2SO_4, filtered, and concentrated in vacuum to give the crude product. The residue was purified by column chromatography on silica gel (PE/EtOAc = 1/1) to the desired product **8** (70 mg, 70%) as a white solid. ^{1}H NMR (400 MHz, DMSO-d_6) δ 11.83 (*s*, 1H), 9.64 (*s*, 1H), 7.85 (*d*, $J = 8.1$ Hz, 2H), 7.46 (*d*, $J = 8.1$ Hz, 2H), 7.00 (*s*, 1H), 5.33 (*s*, 1H), 4.78 (*d*, $J = 6.1$ Hz, 1H), 2.84–2.72 (*m*, 8H), 1.92–1.83 (*m*, 4H), 1.33 (*d*, $J = 6.4$ Hz, 3H).^{13}C NMR (101 MHz, DMSO-d_6) δ 166.0, 152.8, 143.9, 141.3, 131.1, 128.5, 128.5, 125.9, 120.0, 68.2, 33.0, 30.9, 26.1, 25.9. HRMS (ESI) calcd for $C_{21}H_{25}N_2O_4S$ $[M + H]^+$: 401.1535, found 401.1530.

Amino-*N*-(*N*-(1,2,3,5,6,7-hexahydro-s-indacen-4-yl)sulfamoyl)benzamide (11)

To remove the Boc protective group, compound **10** (60 mg, 0.13 mmol) from above was dissolved in 1:2 (v/v) mix of conc. HCl: EtOAc (6 mL) and let stay at rt for 1 h. After concentrated and neutralized with ammonia, the reaction mixture was extracted with DCM (30 mL × 2). The

combined organic phases were then washed with brine (30 mL), dried over anhydrous Na_2SO_4, filtered, and concentrated in vacuum to give the residue. The residue was purified by column chromatography on silica gel (DCM/MeOH = 40/1) to the desired product **11** (46 mg, 97%) as a white solid. ^{1}H NMR (400 MHz, DMSO-d_6) δ 11.29 (*s*, 1H), 9.35 (*s*, 1H), 7.63 (*d*, $J = 8.1$ Hz, 2H), 6.98 (*s*, 1H), 6.53 (*d*, $J = 8.1$ Hz, 2H), 5.94 (*s*, 2H), 2.87–2.71 (*m*, 8H), 1.93–1.79 (*m*, 4H). ^{13}C NMR (151 MHz, DMSO-d_6) δ 165.6, 153.6, 143.8, 141.2, 130.6, 128.8, 119.7, 118.8, 112.9, 33.0, 30.8, 25.8. HRMS (ESI) calcd for $C_{19}H_{22}N_3O_3S$ $[M + H]^+$: 372.1382, found 372.1378.

Acrylamido-*N*-(*N*-(1,2,3,5,6,7-hexahydro-s-indacen-4-yl) sulfamoyl)benzamide (12)

Compound **11** (70 mg, 0.19 mmol) and DIPEA (0.10 mL, 0.57 mmol) were dissolved in dry DMF (3 mL) and the temperature of the solution was lowered to 0 °C. A solution of acryloyl chloride (0.02 mL, 0.23 mmol) was added dropwise. The reaction temperature was increased gradually from 0 °C to room temperature and stirring was continued 3 h at room temperature. Solvent was suspended in 10% HCl (10 mL) and then extracted with DCM (30 mL × 2). The combined organic extracts were washed with sat. $NaHCO_3$ (20 mL), dried over anhydrous Na_2SO_4, and evaporated to give the crude product. The residue was purified by column chromatography on silica gel (PE/EtOAc = 1/1) to the desired product **12** (30 mg, 38%) as a white solid. ^{1}H NMR (400 MHz, DMSO-d_6) δ 11.77 (*s*, 1H), 10.46 (*s*, 1H), 9.58 (*s*, 1H), 7.88 (*d*, $J = 8.3$ Hz, 2H), 7.76 (*d*, $J = 8.5$ Hz, 2H), 6.99 (*s*, 1H), 6.46 (*dd*, $J = 16.8$, 10.1 Hz, 1H), 6.30 (*d*, $J = 16.8$ Hz, 1H), 5.81 (*d*, $J =$ 10.1 Hz, 1H), 2.82–2.72 (*m*, 8H), 1.91–1.82 (*m*, 4H). ^{13}C NMR (151 MHz, DMSO-d_6) δ 165.6, 164.0, 143.9, 143.3, 141.2, 132.0, 130.0, 128.6, 128.2, 127.5, 119.8, 119.1, 33.0, 30.9, 25.8. HRMS (ESI) calcd for $C_{22}H_{24}N_3O_4S$ $[M + H]^+$: 426.1488, found 426.1487.

1-Amino-*N*-(1,2,3,5,6,7-hexahydro-s-indacen-4-yl) cyclopropanecarboxamide (13)

1-Amino cyclopropanecarboxylic acid (100 mg, 0.99 mmol) was dissolved in a mixture of dioxane (3.0 mL) and 0.5-N NaOH (3.0 mL). To this, solution was added di-*tert*-butyl dicarbonate (0.28 mL, 1.5 mmol) and the resulting mixture stirred at rt for 15 h. The reaction mixture was concentrated under reduced pressure, and diluted with EtOAc (30 mL) and 1 N HCl (10 mL). The aqueous solution was extracted with EtOAc (20 mL × 2), and the combined organic phases were washed with brine (30 mL), dried over anhydrous Na_2SO_4, and concentrated under reduced pressure. The residue was purified by column chromatography on silica gel (PE/EtOAc = 1/2), giving pure product (134 mg, 67%) as white solid.

To a stirred suspension of the above compound (134 mg, 0.66 mmol) in DCM (2 mL), EDCI (255 mg, 1.33 mmol), HOBt (180 mg, 1.33 mmol), and triethylamine (0.71 mL, 2 mmol) were added, followed by the compound **1** (114 mg, 0.66 mmol). The clear solution was stirred at room temperature 22 h. The reaction mixture diluted with DCM (30 mL), and washed with 1-N HCl. The aqueous solution was extracted with EtOAc (20 mL × 2), and the combined organic phases were washed with brine (30 mL), dried over anhydrous Na_2SO_4, filtered, and concentrated in vacuum to give the crude product. To remove its Boc protective group, the crude product from above was dissolved in 1:2 (v/v) mix of conc. HCl: EtOAc (6 mL), and let stay at rt for 1 h. After concentrated and neutralized with ammonia, the reaction mixture was extracted with DCM (30 mL × 2). The combined organic phases were then washed with brine (30 mL), dried over anhydrous Na_2SO_4, filtered, and concentrated in vacuum to give the crude product. The residue was purified by column chromatography on silica gel (PE/EtOAc = 1/2) to the desired product **13** (100 mg, 59%) as a white solid. ^{1}H NMR (400 MHz, DMSO-d_6) δ 9.52 (*s*, 1H), 6.92 (*s*, 1H), 2.79 (*t*, $J = 7.0$ Hz, 4H), 2.67 (*t*, $J = 7.0$ Hz, 4H), 2.49 (*s*, 2H), 1.96 (*m*, 4H), 1.11 (*d*, $J =$ 2.8 Hz, 2H), 0.83 (*d*, $J = 2.8$ Hz, 2H).

General procedures (GP2)

To a stirred aromatic compounds (1.5 eq) in DCM (2 mL/mmol), EDCI (1 eq), HOBt (1 eq) and triethylamine (1.5 eq) were added, followed by compound **13** (1 eq).The clear solution was stirred at room temperature 20–24 h. The reaction mixture was diluted with DCM (30 mL), and washed with 1-N HCl and water. The organic layer was dried over anhydrous Na_2SO_4, filtered, and concentrated in vacuum to give the crude product. The residue was purified by column chromatography on silica gel to afford the corresponding products.

4-Fluoro-*N*-(1-((1,2,3,5,6,7-hexahydro-s-indacen-4-yl) carbamoyl)cyclopropyl)benzamide (14)

According to **GP2**, 4-fluorobenzoic acid (51 mg, 0.36 mmol) and compound **13** (55 mg, 0.24 mmol) were converted to the desired product **14** (65 mg, 72%) as a white solid. ^{1}H NMR (400 MHz, DMSO-d_6) δ 9.26 (*s*, 1H), 9.09 (*s*, 1H), 8.00 (*m*, 2H), 7.29 (*t*, $J = 8.5$ Hz, 2H), 6.94 (*s*, 1H), 2.78 (*m*, 4H), 2.64 (*m*, 4H), 2.00–1.86 (*m*, 4H), 1.39 (*s*, 2H), 1.04 (*s*, 2H). ^{13}C NMR (151 MHz, DMSO-d_6) δ 169.9, 167.0, 164.4 (*d*, $J_{C\text{-}F} = 248.70$), 143.0, 138.7, 131.3, 130.7 (*d*, $J_{C\text{-}F} = 8.92$), 130.5, 118.3, 115.3 (*d*, $J_{C\text{-}F} = 21.65$), 35.4, 32.9, 30.6, 25.6, 16.7. HRMS (ESI) calcd for $C_{23}H_{24}FN_2O_2$ $[M + H]^+$: 379.1822, found 379.1819.

N-(1-((1,2,3,5,6,7-hexahydro-s-indacen-4-yl)carbamoyl) cyclopropyl)-4-methylbenzamide(15)

According to **GP2**, *p*-toluic acid (22 mg, 0.16 mmol) and compound **13** (40 mg, 0.16 mmol) were converted to the desired product **15** (20 mg, 33%) as a white solid. ^{1}H NMR (400 MHz, DMSO-d_6) δ 9.20 (*s*, 1H), 8.98 (*s*, 1H), 7.84 (*d*, $J = 7.8$ Hz, 2H), 7.26 (*d*, $J = 7.8$ Hz, 2H), 6.94 (*s*, 1H), 2.79 (*t*, $J = 6.9$ Hz, 4H), 2.66 (*t*, $J = 7.0$ Hz, 4H), 2.35 (*s*, 3H), 2.00–1.85 (*m*, 4H), 1.40 (*d*, $J = 2.5$ Hz, 2H), 1.04 (*d*, $J = 2.5$ Hz, 2H). ^{13}C NMR (151 MHz, DMSO-d_6) δ 170.0, 167.9, 143.0, 141.5, 138.6, 131.9, 130.5, 128.9, 128.2, 118.2, 35.4, 32.9, 30.6, 25.6, 21.4, 16.6. HRMS (ESI) calcd for $C_{24}H_{27}N_2O_2$ $[M + H]^+$: 375.2073, found 375.2070.

N-(1-((1,2,3,5,6,7-hexahydro-s-indacen-4-yl)carbamoyl) cyclopropyl)-4-methoxybenzami-de (16)

According to **GP2**, 4-methoxybenzoic acid (53 mg, 0.35 mmol) and compound **15** (60 mg, 0.24 mmol) were converted to the desired product **19** (78 mg, 83%) as a white solid. ^{1}H NMR (400 MHz, DMSO-d_6) δ 9.19 (*s*, 1H), 8.91 (*s*, 1H), 7.91 (*d*, $J = 8.4$ Hz, 2H), 6.98 (*d*, $J = 8.5$ Hz, 2H), 6.93 (*s*, 1H), 3.80 (*s*, 3H), 2.79 (*t*, $J = 6.9$ Hz, 4H), 2.65 (*t*, $J = 6.9$ Hz, 4H), 1.97–1.87 (*m*, 4H), 1.38 (*d*, $J = 2.2$ Hz, 2H), 1.03 (*d*, $J = 2.2$ Hz, 2H). ^{13}C NMR (151 MHz, DMSO-d_6) δ 174.9, 172.2, 166.8, 147.8, 143.3, 135.3, 134.8, 131.8, 123.0, 118.3, 60.5, 40.1, 37.7, 35.4, 30.3, 21.4. HRMS (ESI) calcd for $C_{24}H_{27}N_2O_3$ $[M + H]^+$: 391.2022, found 391.2015.

((1,2,3,5,6,7-Hexahydro-s-indacen-4-yl)carbamoyl) cyclopropyl)-4-(trifluoromethyl)benzamide (17)

According to **GP2**, 4-(trifluoromethyl)benzoic acid (90 mg, 0.46 mmol) and compound **13** (80 mg, 0.31 mmol) were converted to the desired product **17** (61 mg, 46%) as a white solid. ^{1}H NMR (400 MHz, DMSO-d_6) δ 9.30 (s, 2H), 8.14 (d, $J = 8.0$ Hz, 2H), 7.84 (*d*, $J = 8.1$ Hz, 2H), 6.94 (*s*, 1H), 2.80 (*t*, $J = 7.0$ Hz, 4H), 2.66 (*t*, $J = 7.0$ Hz, 4H), 2.01–1.86 (*m*, 4H), 1.42 (*d*, $J = 2.6$ Hz, 2H), 1.07 (*d*, $J = 2.6$ Hz, 2H). ^{13}C NMR (151 MHz, DMSO-d_6) δ 169.7 (*q*, $J_{C\text{-}F} = 272.99$), 166.8, 143.0, 138.8, 138.5, 131.5 (*q*, $J_{C\text{-}F} = 31.79$), 130.5, 129.1, 125.4 (*q*, $J_{C\text{-}F} = 3.68$), 124.4 (*q*, $J_{C\text{-}F} = 272.56$), 118.3, 35.4, 32.9, 30.6, 25.5, 16.7. HRMS (ESI) calcd for $C_{24}H_{24}F_3N_2O_2$ $[M + H]^+$: 429.1790, found 429.1788.

4-Acetyl-*N*-(1-((1,2,3,5,6,7-hexahydro-s-indacen-4-yl) carbamoyl)cyclopropyl)benzamide (18)

According to **GP2**, 4-acetylbenzoic acid (68 mg, 0.41 mmol) and compound **13** (80 mg, 0.31 mmol) were converted to the desired product **18** (108 mg, 86%) as a white solid. ^{1}H NMR (400 MHz, DMSO-d_6) δ 9.28 (*s*, 1H), 9.24 (*s*, 1H), 8.04 (*dd*, $J = 17.7$, 8.2 Hz, 4H), 6.94 (*s*, 1H), 2.80 (*t*, $J = 6.9$ Hz, 4H), 2.66 (*t*, $J = 7.1$ Hz, 4H), 2.62 (*s*, 3H), 1.95 (*m*, 7.0 Hz, 4H), 1.42 (*d*, $J = 2.3$ Hz, 2H), 1.07 (*d*, $J = 2.4$ Hz, 2H). ^{13}C NMR (151 MHz, DMSO-d_6) δ 198.2, 169.8, 167.2, 143.0, 139.0, 138.8, 138.6, 130.5, 128.5, 128.2, 118.3, 35.5, 32.9, 30.6, 27.4, 25.6, 16.7. HRMS (ESI) calcd for $C_{25}H_{27}N_2O_3$ $[M + H]^+$: 403.2022, found 403.2018.

tert-Butyl(4-((1-((1,2,3,5,6,7-hexahydro-s-indacen-4-yl) carbamoyl)cyclopropyl)carbamoyl)phenyl)carbamate (20)

According to **GP2**, 4-((*tert*-butoxycarbonyl)amino)benzoic acid (138 mg, 0.58 mmol) and compound **13** (100 mg, 0.39 mmol) were converted to the desired product **20** (91 mg, 49%) as a white solid. ^{1}H NMR (400 MHz, DMSO-d_6) δ 9.61 (*s*, 1H), 9.19 (*s*, 1H), 8.91 (*s*, 1H), 7.85 (*d*, $J = 8.4$ Hz, 2H), 7.50 (*d*, $J = 8.4$ Hz, 2H), 6.93 (*s*, 1H), 2.79 (*t*, $J = 6.7$ Hz, 4H), 2.65 (*t*, $J = 6.8$ Hz, 4H), 2.01–1.85 (*m*, 4H), 1.48 (*s*, 9H), 1.38 (*s*, 2H), 1.03 (*s*, 2H). ^{13}C NMR (151 MHz, DMSO-d_6) δ 170.1, 167.5, 153.0, 143.0, 142.8, 138.6, 130.5, 129.0, 128.0, 118.2, 117.2, 79.9, 35.4, 32.9, 30.6, 28.5, 25.6, 16.6. HRMS (ESI) calcd for $C_{28}H_{34}N_3O_4$ $[M + H]^+$: 476.2549, found 476.2547.

N-(1-((1,2,3,5,6,7-hexahydro-s-indacen-4-yl)carbamoyl) cyclopropyl)-5-(2-hydroxypropan-2-yl)furan-2-carboxamide (23)

To a solution of *i*-propylamine (0.12 mL, 0.99 mmol) in THF (1 mL) was added 2.4 *n*-butyllithium (0.33 mL, 0.99 mol) in hexanes at −15 to −8 °C with stirring under a nitrogen atmosphere. The mixture was diluted with THF (1 mL) and cooled to −74 °C. The furan-2-carboxylic acid (50 mg, 0.45 mmol) in THF (1 mL) was added so as to keep the temperature at −70 to −77 °C. After 30 min in the cold, acetone (28 mg, 0.50 mmol) in THF (1 mL) was added dropwise while keeping the temperature below −70 °C, and then the reaction mixture was allowed to come to room temperature. The mixture was quenched with water, and most of the THF was removed by evaporation under vacuum. The aqueous residue was extracted with diethylether (20 mL × 2) and acidified with 5-N HCl. The product was extracted with diethylether (30 mL × 3), dried with anhydrous Na_2SO_4, and concentrated to give crude 4-(2-hydroxypropan-2-yl)furan-2-carboxylic acid as an oil (50 mg, 65%).

According to **GP2**, the above 4-(2-hydroxypropan-2-yl) furan-2-carboxylic acid (50 mg, 0.29 mmol) and compound **13** (51.2 mg, 0.2 mmol) were converted to the desired product **23** (22 mg, 27%) as a white solid. ^{1}H NMR (400 MHz, $CDCl_3$) δ 8.28 (*s*, 1H), 7.37 (*s*, 1H), 7.28 (*s*, 1H), 7.12 (*s*,

1H), 6.98 (*s*, 1H), 6.32 (*s*, 1H), 2.87 (*t*, $J = 7.0$ Hz, 4H), 2.78 (*t*, $J = 6.3$ Hz, 4H), 2.13–1.99 (*m*, 4H), 1.70 (*s*, 2H), 1.61 (*s*, 6H), 1.18 (*s*, 2H). ^{13}C NMR (151 MHz, $CDCl_3$) δ 169.5, 169.3, 149.3, 143.9, 137.1, 134.3, 129.5, 129.0, 118.5, 116.3, 115.2, 111.3, 77.2, 77.0, 76.8, 36.2, 32.9, 30.8, 29.7, 25.6, 16.8. HRMS (ESI) calcd for $C_{24}H_{29}N_2O_4$ $[M + H]^+$: 409.2127, found 409.2122.

(1-((1,2,3,5,6,7-hexahydro-s-indacen-4-yl)carbamoyl) cyclopropyl)-4-(2-hydroxypropan-2-yl)benzamide (24)

4-Isopropylbenzoic acid (100 mg, 0.60 mmol) was dissolved in a solution of potassium hydroxide (82 mg, 1.46 mmol) in water (2.5 mL). To the reaction mixture was added a solution of potassium permanganate (192 mg, 1.21 mmol) in water (2.5 mL). The combined mixture was allowed to stir at 60 °C for 2 h. The reaction mixture was cooled to 0 °C and treated with ethylene glycol and cooled to 0 °C. The solid were removed by filtration and the filtrate was acidified to pH 1 by addition of 6-N HCl solution. The solid was removed by filtration, and the fitrate was extracted with diethylether (30 mL × 2). The combined organic extracts were dried over anhydrous Na_2SO_4, filtered, and concentrated in vacuo. The residue was purified by column chromatography on silica gel (PE/EtOAc = 1/1), giving 4 (2-hydroxypropan-2-yl)benzoic acid (102 mg, 42%) as a white solid.

According to **GP2**, the above 4-(2-hydroxypropan-2-yl) benzoic acid (102 mg, 0.56 mmol) and compound **13** (96 mg, 0.38 mmol) were converted to the desired product **24** (52 mg, 33%) as a white solid. ^{1}H NMR (400 MHz, DMSO-d_6) δ 9.20 (*s*, 1H), 8.99 (*s*, 1H), 7.88 (*d*, $J = 8.1$ Hz, 2H), 7.52 (*d*, $J = 8.2$ Hz, 2H), 6.93 (*s*, 1H), 5.13 (*s*, 1H), 2.79 (*t*, $J = 6.9$ Hz, 4H), 2.66 (*t*, $J = 6.9$ Hz, 4H), 2.01–1.86 (*m*, 4H), 1.42 (*s*, 6H),1.40 (*d*, $J = 2.5$ Hz, 2H) 1.04 (*d*, $J = 2.2$ Hz, 2H). ^{13}C NMR (151 MHz, DMSO-d_6) δ 170.0, 167.9, 154.3, 143.0, 138.6, 132.4, 130.5, 127.8, 124.5, 118.2, 71.2, 35.4, 32.9, 32.3, 30.6, 25.6, 16.6. HRMS (ESI) calcd for $C_{26}H_{31}N_2O_3$ $[M + H]^+$: 419.2335, found 419.2334.

Methyl 3-((1-((1,2,3,5,6,7-hexahydro-s-indacen-4-yl) carbamoyl)cyclopropyl)carbamoyl-benzoate (25)

According to **GP2**, 3-(methoxycarbonyl)benzoic acid (104 mg, 0.58 mmol) and compound **13** (100 mg, 0.4 mmol) were converted to the desired product **25** (152 mg, 89%) as a white solid. ^{1}H NMR (400 MHz, DMSO-d_6) δ 9.31 (*s*, 1H), 9.28 (*s*, 1H), 8.54 (*s*, 1H), 8.20 (*d*, $J = 7.4$ Hz, 1H), 8.10 (*d*, $J = 7.4$ Hz, 1H), 7.62 (*t*, $J = 7.6$ Hz, 1H), 6.94 (*s*, 1H), 3.89 (*s*, 3H), 2.79 (*m*, 4H), 2.66 (*m*, 4H), 2.00–1.86 (*m*, 4H), 1.40 (*s*, 2H), 1.06 (*s*, 2H). ^{13}C NMR (151 MHz, DMSO-d_6) δ 170.4, 168.1, 152.2, 143.0, 138.3, 130.5, 129.7, 121.3, 118.1, 112.7, 35.4, 32.9, 30.6, 25.6, 16.6. HRMS (ESI) calcd for $C_{25}H_{27}N_2O_4$ $[M + H]^+$: 419.1971, found 419.1969.

3-Bromo-*N*-(1-((1,2,3,5,6,7-hexahydro-s-indacen-4-yl) carbamoyl)cyclopropyl)benzamide (27)

According to **GP2**, 3-bromobenzoic acid (86 mg, 0.43 mmol) and compound **13** (74 mg, 0.29 mmol) were converted to the desired product **25** (76 mg, 60%) as a white solid. ^{1}H NMR (400 MHz, DMSO-d_6) δ 9.30 (*s*, 1H), 9.18 (*s*, 1H), 8.16 (*s*, 1H), 7.91 (*d*, $J = 7.6$ Hz, 1H), 7.73 (*d*, $J = 7.8$ Hz, 1H), 7.43 (*t*, $J = 7.8$ Hz, 1H), 6.95 (*s*, 1H), 2.80 (t, $J = 6.9$ Hz, 4H), 2.66 (*t*, $J = 7.0$ Hz, 4H), 2.01–1.88 (*m*, 4H), 1.40 (*d*, $J = 2.4$ Hz, 2H), 1.05 (*d*, $J = 2.4$ Hz, 2H).^{13}C NMR (151 MHz, DMSO-d_6) δ 169.8, 166.6, 143.0, 138.8, 137.0, 134.3, 131.0, 130.7, 130.5, 127.3, 121.8, 118.3, 35.4, 33.0, 30.6, 25.6, 16.6. HRMS (ESI) calcd for $C_{23}H_{24}BrN_2O_2$ $[M + H]^+$: 439.1021, found 439.1021.

Acetyl-*N*-(1-((1,2,3,5,6,7-hexahydro-s-indacen-4-yl) carbamoyl)cyclopropyl)benzamide (19)

Compound **18** (70 mg, 0.17 mmol) was dissolved in 2 ml of ethanol and sodium borohydride (34 mg, 0.90 mg) was added to the mixture. The reaction was refluxed at 80 °C for 12 h. The reaction mixture was diluted with 30 mL of dichloromethane, and washed with brine. The organic layer was dried over anhydrous Na_2SO_4, filtered, and concentrated in vacuum to give the crude product. The residue was purified by column chromatography on silica gel (PE/EtOAc = 1/2) to the desired product **19** (29 mg, 42%) as a white solid. ^{1}H NMR (400 MHz, DMSO-d_6) δ 9.20 (*s*, 1H), 9.00 (*s*, 1H), 7.89 (*d*, $J = 7.9$ Hz, 2H), 7.40 (*d*, $J = 8.0$ Hz, 2H), 6.94 (*s*, 1H), 5.27 (*d*, $J = 4.0$ Hz, 1H), 4.84–4.70 (*m*, 1H), 2.79 (*t*, $J = 6.9$ Hz, 4H), 2.66 (*t*, $J = 7.0$ Hz, 4H), 1.98–1.89 (*m*, 4H), 1.40 (*d*, $J = 2.2$ Hz, 2H), 1.31 (*d*, $J = 6.3$ Hz, 3H), 1.04 (*d*, $J = 2.3$ Hz, 2H). ^{13}C NMR (151 MHz, DMSO-d_6) δ 170.0, 167.9, 151.2, 143.02, 138.6, 133.0, 130.5, 128.0, 125.2, 118.2, 68.2, 40.4, 40.2, 40.1, 40.0, 39.8, 39.7, 39.5, 35.4, 32.9, 30.6, 26.4, 25.6, 16.6. HRMS (ESI) calcd for$C_{25}H_{29}N_2O_3$ $[M + H]^+$: 405.2178, found 405.2178.

Amino-*N*-(1-((1,2,3,5,6,7-hexahydro-s-indacen-4-yl) carbamoyl)cyclopropyl)benzamide (21)

To remove the Boc protective group, the compound **20** (100 mg, 0.21 mmol) was dissolved in 6 mL 1:2 (v/v) mix of conc. HCl:EtOAc and let stay at rt for 1 h. It was then concentrated down on rotovap and then on high vacuum. After neutralizing with ammonia, the reaction mixture was diluted with DCM (30 mL × 2), and washed with brine. The

organic layer was dried over Na_2SO_4, filtered, and concentrated in vacuum to give the crude product. The residue was purified by column chromatography on silica gel (PE/EtOAc = 1/2) to the desired product **21** (72 mg, 91%) as a white solid. ^{1}H NMR (400 MHz, DMSO-d_6) δ 9.10 (*s*, 1H), 8.60 (*s*, 1H), 7.65 (*d*, J = 8.3 Hz, 2H), 6.92 (*s*, 1H), 6.53 (*d*, J = 8.4 Hz, 2H), 5.63 (*s*, 2H), 2.79 (*t*, J = 6.9 Hz, 4H), 2.65 (*t*, J = 7.0 Hz, 4H), 1.97–1.83 (*m*, 4H), 1.36 (*d*, J = 2.5 Hz, 2H), 0.99 (*d*, J = 2.5 Hz, 2H). ^{13}C NMR (151 MHz, DMSO-d_6) δ 170.4, 168.1, 152.2, 143.0, 138.3, 130.5, 129.7, 121.3, 118.1, 112.7, 35.4, 32.9, 30.6, 25.6, 16.6. HRMS (ESI) calcd for $C_{23}H_{26}N_3O_2$ $[M + H]^+$: 376.2025, found 376.2024.

4-Acrylamido-*N*-(1-((1,2,3,5,6,7-hexahydro-s-indacen-4-yl) carbamoyl)cyclopropyl)benzamide (22)

Compound **21** (106 mg, 0.28 mmol) and DIPEA (0.10 mL, 0.57 mmol) were dissolved in dry DMF (2 mL) and the temperature of the solution was lowered to 0 °C. A solution of acryloyl chloride (0.03 mL, 0.31 mmol) was added dropwise. The reaction temperature was increased gradually from 0 °C to room temperature and stirring was continued 3 h at room temperature. Solvent was suspended in 10% HCl (10 mL) and then extracted with DCM (30 mL × 2). The combined organic extracts were washed with saturated solution of Na_2CO_3 (20 mL), dried over anhydrous Na_2SO_4, and evaporated to give the crude product. The residue was purified by column chromatography on silica gel (DCM/MeOH = 40/1) to the desired product **22** (62 mg, 52%) as a white solid. ^{1}H NMR (400 MHz, DMSO-d_6) δ 10.37 (*s*, 1H), 9.22 (*s*, 1H), 8.97 (*s*, 1H), 7.92 (*d*, J = 8.4 Hz, 2H), 7.73 (*d*, J = 8.5 Hz, 2H), 6.94 (*s*, 1H), 6.45 (*dd*, J = 16.9, 10.1 Hz, 1H), 6.29 (*d*, J = 16.1 Hz, 1H), 5.79 (*d*, J = 11.0 Hz, 1H), 2.79 (*t*, J = 6.8 Hz, 4H), 2.66 (*t*, J = 6.9 Hz, 4H), 2.02–1.87 (*m*, 4H), 1.39 (*d*, J = 2.2 Hz, 2H), 1.04 (*d*, J = 2.2 Hz, 2H). ^{13}C NMR (151 MHz, DMSO-d_6) δ 174.8, 172.1, 168.6, 147.8, 146.8, 143.4, 136.8, 135.3, 134.3, 133.9, 132.7, 123.4, 123.0, 45.2, 45.1, 45.0, 44.8, 44.7, 44.5, 44.4, 44.3, 40.1, 37.7, 35.4, 30.3, 21.4. HRMS (ESI) calcd for $C_{26}H_{28}N_3O_3$ $[M + H]^+$: 430.2131, found 430.2127.

3-((1-((1,2,3,5,6,7-hexahydro-s-indacen-4-yl)carbamoyl) cyclopropyl)carbamoyl)benzoic acid (26)

Compound **25** (100 mg, 0.24 mmol) was dissolved in THF, and then dissolved lithium hydroxide (11.5 mg, 0.48 mmol) in water was added dropwise into the above mixture and stirred at room temperature for 2 h. Spin dry THF, add citric acid to neutralize to weak acidity. The reaction mixture was diluted with DCM (30 mL × 2), and washed with brine. The organic layer was dried over anhydrous Na_2SO_4, filtered, and concentrated in vacuum to give the crude product. The residue was purified by column chromatography on silica gel (DCM/MeOH = 40/1) to the desired product **26** (47 mg, 48%) as a white solid. ^{1}H NMR (400 MHz, DMSO-d_6) δ 13.07 (*s*, 1H), δ 9.30 (*s*, 1H), 9.25 (*s*, 1H), 8.53 (*s*, 1H), 8.16 (*d*, J = 7.6 Hz, 1H), 8.07 (*d*, J = 7.6 Hz, 1H), 7.58 (*t*, J = 7.7 Hz, 1H), 6.94 (*s*, 1H), 2.79 (*t*, J = 6.9 Hz, 4H), 2.66 (*t*, J = 7.0 Hz, 4H), 1.99–1.89 (*m*, 4H), 1.40 (*s*, 2H), 1.06 (*d*, J = 2.4 Hz, 2H). ^{13}C NMR (151 MHz, DMSO-d_6) δ 169.9, 167.5, 167.3, 143.0, 138.8, 135.2, 132.4, 132.2, 131.2, 130.5, 129.2, 128.7, 118.3, 35.4, 33.0, 30.6, 25.6, 16.7. HRMS (ESI) calcd for $C_{24}H_{25}N_2O_4$ $[M + H]^+$: 405.1814, found 405.1815.

N-(1-((1,2,3,5,6,7-hexahydro-s-indacen-4-yl)carbamoyl) cyclopropyl)-3-(methylamino)benzamide (28)

A magnetic stirrer bar, compound **27** (50 mg, 0.11 mmol), methylamine (2.2 mL, 16 mmol, a 40% aqueous solution), and copper powder (4 mg, 0.006 mmol) were added to a screw-capped tube (15 mL) under air. The reaction mixture was stirred and heated at 100 °C, and the mixture was reacted for 22 h. Spin dry under vacuum. The residue was purified by column chromatography on silica gel (PE/EtOAc = 1.5/1) to the desired product **28** (19 mg, 43%) as yellow oil. ^{1}H NMR (400 MHz, $CDCl_3$) δ 8.36 (*s*, 1H), 7.24 (*t*, J = 7.8 Hz, 1H), 7.09 (*s*, 1H), 7.05–6.96 (*m*, 2H), 6.77 (*d*, J = 7.9 Hz, 1H), 2.88 (*m*, 7H), 2.80 (*t*, J = 7.1 Hz, 4H), 2.11–1.99 (*m*, 4H), 1.73 (*s*, 2H), 1.18 (*s*, 2H). ^{13}C NMR (151 MHz, $CDCl_3$) δ 169.5, 169.3, 149.3, 143.9, 137.1, 134.3, 129.5, 129.0, 118.5, 116.3, 115.2, 111.3, 77.2, 77.0, 76.8, 36.2, 32.9, 30.8, 29.7, 25.6, 16.8. HRMS (ESI) calcd for $C_{24}H_{28}N_3O_2$ $[M + H]^+$: 390.2182, found 390.2176.

(1,2,3,5,6,7-Hexahydro-s-indacen-4-yl)-1-(4-methoxyphenylsulfonamido)cyclopropanecarboxamide (29)

Into a 50-mL round-bottom flask equipped with a magnetic stir bar and under nitrogen was weighted 4-methoxybenzene-1-sulfonyl chloride (62 mg, 0.3 mmol) in dichloromethane (10 mL). The suspension was cooled to 0 °C and then compound **13** (50 mg, 0.2 mmol) was added, followed by the addition of pyridine (0.03 mL, 0.4 mmol). The resulting suspension was stirred at room temperature for 16 h. The reaction mixture was poured into a 60-mL separatory funnel and washed with 1-N aqueous HCl solution (20 mL), water (20 mL), and brine (20 mL). The organic layer was dried over anhydrous Na_2SO_4, filtered, and concentrated under reduced pressure. Purification by column chromatography through silica gel, eluting with 100% DCM to 5% MeOH in DCM as a gradient afforded compound **29** as a white solid (48 mg, 56%). ^{1}H NMR (400 MHz, DMSO-d_6) δ 8.96 (*s*, 1H), 8.58 (*s*, 1H), 7.74 (*d*,

$J = 8.0$ Hz, 2H), 7.11 (*d*, $J = 8.1$ Hz, 2H), 6.95 (*s*, 1H), 3.83 (*s*, 3H), 2.80 (*t*, $J = 6.7$ Hz, 4H), 2.61 (*t*, $J = 6.8$ Hz, 4H), 1.96 (*dd*, $J =$ m, 4H), 1.15 (*s*, 2H), 0.81 (*s*, 2H). ^{13}C NMR (151 MHz, DMSO-d_6) δ 169.5, 162.8, 143.2, 138.0, 133.8, 130.1, 129.1, 118.3, 114.8, 56.1, 36.7, 32.9, 30.6, 25.6, 14.5. HRMS (ESI) calcd for $C_{23}H_{27}N_2O_4S$ $[M + H]^+$: 427.1692, found 427.1685.

N-(1,2,3,5,6,7-hexahydro-s-indacen-4-yl)-1-(4-(trifluoromethyl)phenylsulfonamido) cyclopropanecarboxamide (30)

Into a 50-mL round-bottom flask equipped with a magnetic stir bar and under nitrogen was weighted 4-(trifluoromethyl) benzene-1-sulfonyl chloride (75 mg, 0.3 mmol) in DCM (10 mL). The suspension was cooled to 0 °C and then compound **13** (50 mg, 0.2 mmol) was added, followed by the addition of pyridine (0.03 mL, 0.4 mmol). The resulting suspension was stirred at room temperature for 16 h. The reaction mixture was poured into a 60-mL separatory funnel and washed with 1-N aqueous HCl solution (3×20 mL), water (20 mL), and brine (20 mL). The organic layer was dried over anhydrous Na_2SO_4, filtered, and concentrated under reduced pressure. Purification by column chromatography through silica gel, eluting with 100% DCM to 2.5% MeOH in DCM as a gradient afforded compound **30** as a white solid (39 mg, 45%). ^{1}H NMR (400 MHz, DMSO-d_6) δ 9.04 (*s*, 1H), 8.99 (*s*, 1H), 8.01 (*dd*, $J = 15.4$, 8.0 Hz, 4H), 6.94 (*s*, 1H), 2.78 (*m*, 4H), 2.55 (*m*, 4H), 1.98–1.89 (*m*, 4H), 1.23 (*s*, 2H), 0.87 (*s*, 2H).^{13}C NMR (151 MHz, DMSO-d_6) δ 169.1, 146.3, 143.2, 138.2, 132.7 (*q*, $J_{C\text{-}F} = 32.09$) 130.0, 128.0, 127.0 (*q*, $J_{C\text{-}F} = 3.78$), 124.5 (*q*, $J_{C\text{-}F} = 272.49$), 118.4, 36.8, 32.9, 30.5, 25.5, 14.7. HRMS (ESI) calcd for $C_{23}H_{24}F_3N_2O_3S$ $[M + H]^+$: 465.1460, found 465.1456.

Cell culture

BV-2 murine microglia cells were grown in DMEM supplemented with 10% heat-inactivated FBS, penicillin (100 U/ml), streptomycin (10 µg/ml), and 5% CO_2 at 37 °C. Rat primary microglia were isolated from 1- to 2-day-old neonatal Sprague-Dawley rats as described previously [50]. In brief, the chopped cerebral cortex were digested with papain (2 mg/ml) 37 °C for 30 min and then mechanistically dissociated using different pore size of tips and cell strainer (40 µM). The cells were seeded in poly-D-lysine-coated 75-mm flasks and cultured at 37 °C, 5% CO_2. Fourteen days after culturing, the microglia cells were collected by shaking and centrifugation. Murine BMDM were prepared from femoral bone marrow cells as described previously [37]. In brief, bone marrow cells were obtained by flushing method. After removing contaminated red cells using erythrocytes lysis buffer, the remaining bone marrow cells were incubated in complete medium with 50-mg/ml recombinant mouse M-CSF for 7 days. Animal study was approved by Institutional Review Board of Soochow University and was performed in accordance with the guidelines published in the National Institutes of Health.

Cell viability test

BV-2 microglia cell viability was measured by MTT reagent as described previously [50].

Enzyme-linked immunosorbent assay (ELISA)

The levels of IL-1β or TNF-α in the supernatants of cells were measured by IL-1β or TNF-α specific ELISA kit according to the instruction of the manufacturer [50].

Nitrite quantification

The levels of NO in the supernatants of cells were detected using Griess reagent as described previously [47, 48].

Acknowledgements This work was supported by the National Natural Science Foundation of China (31970909, 81703330, and 81372688), the Natural Science Foundation of Jiangsu Province (BK20170347), the Priority Academic Program Development of the Jiangsu Higher Education Institutes (PAPD), Suzhou Municipal Science and Technology Bureau (SYS2020092), and the Jiangsu Key Laboratory of Neuropsychiatric Diseases (BM2013003).

Compliance with ethical standards

Conflict of interest The authors declare no competing interests.

References

1. Weed DL. The merger of bioethics and epidemiology. J Clin Epidemiol. 1991;44:15S–22S.
2. Block ML, Zecca L, Hong JS. Microglia-mediated neurotoxicity: uncovering the molecular mechanisms. Nat Rev Neurosci. 2007;8:57–69. https://doi.org/10.1038/nrn2038.
3. Dinarello CA. Immunological and inflammatory functions of the interleukin-1 family. Annu Rev Immunol. 2009;27:519–50. https://doi.org/10.1146/annurev.immunol.021908.132612.
4. Wen H, Miao EA, Ting JP. Mechanisms of NOD-like receptor-associated inflammasome activation. Immunity. 2013;39:432–41. https://doi.org/10.1016/j.immuni.2013.08.037.
5. Prochnicki T, Latz E. Inflammasomes on the crossroads of innate immune recognition and metabolic control. Cell Metab. 2017;26:71–93. https://doi.org/10.1016/j.cmet.2017.06.018.
6. Baldwin AG, Brough D, Freeman S. Inhibiting the inflammasome: a chemical perspective. J Med Chem. 2016;59:1691–710. https://doi.org/10.1021/acs.jmedchem.5b01091.
7. Mangan MSJ, Olhava EJ, Roush WR, Seidel HM, Glick GD, Latz E. Targeting the NLRP3 inflammasome in inflammatory diseases.

Nat Rev Drug Discov. 2018;17:588–606. https://doi.org/10.1038/nrd.2018.97.
8. Martinon F, Petrilli V, Mayor A, Tardivel A, Tschopp J. Gout-associated uric acid crystals activate the NALP3 inflammasome. Nature. 2006;440:237–41. https://doi.org/10.1038/nature04516.
9. Mastrocola R, Penna C, Tullio F, Femmino S, Nigro D, Chiazza F, et al. Pharmacological Inhibition of NLRP3 inflammasome attenuates myocardial ischemia/reperfusion injury by activation of RISK and mitochondrial pathways. Oxid Med Cell Longev. 2016;2016:5271251. https://doi.org/10.1155/2016/5271251.
10. Broderick L, De Nardo D, Franklin BS, Hoffman HM, Latz E. The inflammasomes and autoinflammatory syndromes. Annu Rev Pathol. 2015;10:395–424. https://doi.org/10.1146/annurev-pathol-012414-040431.
11. Davis BK, Wen H, Ting JP. The inflammasome NLRs in i mmunity, inflammation, and associated diseases. Annu Rev Immunol. 2011;29:707–35. https://doi.org/10.1146/annurev-immunol-031210-101405.
12. Duewell P, Kono H, Rayner KJ, Sirois CM, Vladimer G, Bauernfeind FG, et al. NLRP3 inflammasomes are required for atherogenesis and activated by cholesterol crystals. Nature. 2010;464:1357–61. https://doi.org/10.1038/nature08938.
13. Chen G, Shaw MH, Kim YG, Nunez G. NOD-like receptors: role in innate immunity and inflammatory disease. Annu Rev Pathol. 2009;4:365–98. https://doi.org/10.1146/annurev.pathol.4.110807.092239.
14. Wang S, Yuan YH, Chen NH, Wang HB. The mechanisms of NLRP3 inflammasome/pyroptosis activation and their role in Parkinson's disease. Int Immunopharmacol. 2019;67:458–64. https://doi.org/10.1016/j.intimp.2018.12.019.
15. Huang Y, Jiang H, Chen Y, Wang X, Yang Y, Tao J, et al. Tranilast directly targets NLRP3 to treat inflammasome-driven diseases. EMBO Mol Med. 2018;10. https://doi.org/10.15252/emmm.201708689.
16. Jiang H, He H, Chen Y, Huang W, Cheng J, Ye J, et al. Identification of a selective and direct NLRP3 inhibitor to treat inflammatory disorders. J Exp Med. 2017;214:3219–38. https://doi.org/10.1084/jem.20171419.
17. He H, Jiang H, Chen Y, Ye J, Wang A, Wang C, et al. Oridonin is a covalent NLRP3 inhibitor with strong anti-inflammasome activity. Nat Commun. 2018;9:2550. https://doi.org/10.1038/s41467-018-04947-6.
18. Yin J, Zhao F, Chojnacki JE, Fulp J, Klein WL, Zhang S, et al. NLRP3 inflammasome inhibitor ameliorates amyloid pathology in a mouse model of Alzheimer's disease. Mol Neurobiol. 2018;55:1977–87. https://doi.org/10.1007/s12035-017-0467-9.
19. Gordon R, Albornoz EA, Christie DC, Langley MR, Kumar V, Mantovani S, et al. Inflammasome inhibition prevents alpha-synuclein pathology and dopaminergic neurodegeneration in mice. Sci Transl Med. 2018;10. https://doi.org/10.1126/scitranslmed.aah4066.
20. Yang F, Wang Z, Wei X, Han H, Meng X, Zhang Y, et al. NLRP3 deficiency ameliorates neurovascular damage in experimental ischemic stroke. J Cereb Blood Flow Metab. 2014;34:660–7. https://doi.org/10.1038/jcbfm.2013.242.
21. Mao Q, Qin WZ, Zhang A, Ye N. Recent advances in dopaminergic strategies for the treatment of Parkinson's disease. Acta Pharm Sin. 2020;41:471–82. https://doi.org/10.1038/s41401-020-0365-y.
22. Ren ZX, Zhao YF, Cao T, Zhen XC. Dihydromyricetin protects neurons in an MPTP-induced model of Parkinson's disease by suppressing glycogen synthase kinase-3 beta activity. Acta Pharm Sin. 2016;37:1315–24. https://doi.org/10.1038/aps.2016.42.
23. Schwaid AG, Spencer KB. Strategies for targeting the NLRP3 inflammasome in the clinical and preclinical space. J Med Chem. 2020. https://doi.org/10.1021/acs.jmedchem.0c01307.
24. Dai Z, Chen XY, An LY, Li CC, Zhao N, Yang F, et al. Development of novel tetrahydroquinoline inhibitors of NLRP3 inflammasome for potential treatment of DSS-induced mouse colitis. J Med Chem. 2020. https://doi.org/10.1021/acs.jmedchem.0c01924.
25. Chen Y, He H, Jiang H, Li L, Hu Z, Huang H, et al. Discovery and optimization of 4-oxo-2-thioxo-thiazolidinones as NOD-like receptor (NLR) family, pyrin domain-containing protein 3 (NLRP3) inhibitors. Bioorg Med Chem Lett. 2020;30:127021. https://doi.org/10.1016/j.bmcl.2020.127021.
26. Perregaux DG, McNiff P, Laliberte R, Hawryluk N, Peurano H, Stam E, et al. Identification and characterization of a novel class of interleukin-1 post-translational processing inhibitors. J Pharm Exp Ther. 2001;299:187–97.
27. Dempsey C, Rubio Araiz A, Bryson KJ, Finucane O, Larkin C, Mills EL, et al. Inhibiting the NLRP3 inflammasome with MCC950 promotes non-phlogistic clearance of amyloid-beta and cognitive function in APP/PS1 mice. Brain Behav Immun. 2017;61:306–16. https://doi.org/10.1016/j.bbi.2016.12.014.
28. Coll RC, Robertson AA, Chae JJ, Higgins SC, Munoz-Planillo R, Inserra MC, et al. A small-molecule inhibitor of the NLRP3 inflammasome for the treatment of inflammatory diseases. Nat Med. 2015;21:248–55. https://doi.org/10.1038/nm.3806.
29. van Hout GP, Bosch L, Ellenbroek GH, de Haan JJ, van Solinge WW, Cooper MA, et al. The selective NLRP3-inflammasome inhibitor MCC950 reduces infarct size and preserves cardiac function in a pig model of myocardial infarction. Eur Heart J. 2017;38:828–36. https://doi.org/10.1093/eurheartj/ehw247.
30. van der Heijden T, Kritikou E, Venema W, van Duijn J, van Santbrink PJ, Slutter B, et al. NLRP3 inflammasome inhibition by MCC950 reduces atherosclerotic lesion development in apolipoprotein E-deficient mice-brief report. Arterioscler Thromb Vasc Biol. 2017;37:1457–61. https://doi.org/10.1161/ATVBAHA.117.309575.
31. Ren H, Kong Y, Liu Z, Zang D, Yang X, Wood K, et al. Selective NLRP3 (pyrin domain-containing protein 3) inflammasome inhibitor reduces brain injury after intracerebral hemorrhage. Stroke. 2018;49:184–92. https://doi.org/10.1161/STROKEAHA.117.018904.
32. Primiano MJ, Lefker BA, Bowman MR, Bree AG, Hubeau C, Bonin PD, et al. Efficacy and pharmacology of the NLRP3 inflammasome inhibitor CP-456,773 (CRID3) in murine models of dermal and pulmonary inflammation. J Immunol. 2016;197:2421–33. https://doi.org/10.4049/jimmunol.1600035.
33. Peterson LA. Reactive metabolites in the biotransformation of molecules containing a furan ring. Chem Res Toxicol. 2013;26:6–25. https://doi.org/10.1021/tx3003824.
34. Jochheim CM, Davis MR, Baillie KM, Ehlhardt WJ, Baillie TA. Glutathione-dependent metabolism of the antitumor agent sulofenur. Evidence for the formation of p-chlorophenyl isocyanate as a reactive intermediate. Chem Res Toxicol. 2002;15:240–8.
35. Salla M, Butler MS, Massey NL, Reid JC, Cooper MA, Robertson AAB. Synthesis of deuterium-labelled analogues of NLRP3 inflammasome inhibitor MCC950. Bioorg Med Chem Lett. 2018;28:793–5. https://doi.org/10.1016/j.bmcl.2017.12.054.
36. Salla M, Butler MS, Pelingon R, Kaeslin G, Croker DE, Reid JC, et al. Identification, synthesis, and biological evaluation of the major human metabolite of NLRP3 inflammasome inhibitor MCC950. ACS Med Chem Lett. 2016;7:1034–8. https://doi.org/10.1021/acsmedchemlett.6b00198.
37. Hill JR, Coll RC, Sue N, Reid JC, Dou J, Holley CL, et al. Sulfonylureas as concomitant insulin secretagogues and NLRP3 inflammasome inhibitors. ChemMedChem. 2017;12:1449–57. https://doi.org/10.1002/cmdc.201700270.
38. Agarwal S, Sasane S, Shah HA, Pethani JP, Deshmukh P, Vyas V, et al. Discovery of N-Cyano-sulfoximineurea derivatives as potent

and orally bioavailable NLRP3 inflammasome inhibitors. ACS Med Chem Lett. 2020;11:414–8. https://doi.org/10.1021/acsmedchemlett.9b00433.
39. Hill JR, Coll RC, Schroder K, Robertson AAB. Design, synthesis and evaluation of an NLRP3 inhibitor diazirine photoaffinity probe. Tetrahedron Lett. 2020;61:151849. https://doi.org/10.1016/j.tetlet.2020.151849.
40. Harrison D, Boutard N, Brzozka K, Bugaj M, Chmielewski S, Cierpich A, et al. Discovery of a series of ester-substituted NLRP3 inflammasome inhibitors. Bioorg Med Chem Lett. 2020;30:127560. https://doi.org/10.1016/j.bmcl.2020.127560.
41. Talele TT. The "Cyclopropyl Fragment" is a versatile player that frequently appears in preclinical/clinical drug molecules. J Med Chem. 2016;59:8712–56. https://doi.org/10.1021/acs.jmedchem.6b00472.
42. Savka RD, Plenio H. A hexahydro-s-indacene based NHC ligand for olefin metathesis catalysts. J Organomet Chem. 2012;710:68–74.
43. Kelder J, Grootenhuis PD, Bayada DM, Delbressine LP, Ploemen JP. Polar molecular surface as a dominating determinant for oral absorption and brain penetration of drugs. Pharm Res. 1999;16:1514–9. https://doi.org/10.1023/a:1015040217741.
44. Franchi L, Munoz-Planillo R, Nunez G. Sensing and reacting to microbes through the inflammasomes. Nat Immunol. 2012;13:325–32. https://doi.org/10.1038/ni.2231.
45. Schumann RR, Belka C, Reuter D, Lamping N, Kirschning CJ, Weber JR, et al. Lipopolysaccharide activates caspase-1 (interleukin-1-converting enzyme) in cultured monocytic and endothelial cells. Blood. 1998;91:577–84.
46. Zhang Y, Gu R, Jia J, Hou T, Zheng LT, Zhen X. Inhibition of macrophage migration inhibitory factor (MIF) tautomerase activity suppresses microglia-mediated inflammatory responses. Clin Exp Pharm Physiol. 2016;43:1134–44. https://doi.org/10.1111/1440-1681.12647.
47. Xu Z, Wu J, Zheng J, Ma H, Zhang H, Zhen X, et al. Design, synthesis and evaluation of a series of non-steroidal anti-inflammatory drug conjugates as novel neuroinflammatory inhibitors. Int Immunopharmacol. 2015;25:528–37. https://doi.org/10.1016/j.intimp.2015.02.033.
48. Wu J, Du J, Gu R, Zhang L, Zhen X, Li Y, et al. Inhibition of neuroinflammation by synthetic androstene derivatives incorporating amino acid methyl esters on activated BV-2 microglia. ChemMedChem. 2015;10:610–6. https://doi.org/10.1002/cmdc.201500027.
49. Tao L, Zhang F, Hao L, Wu J, Jia J, Liu JY, et al. 1-O-tigloyl-1-O-deacetyl-nimbolinin B inhibits LPS-stimulated inflammatory responses by suppressing NF-kappaB and JNK activation in microglia cells. J Pharm Sci. 2014;125:364–74.
50. Han CJ, Zheng JY, Sun L, Yang HC, Cao ZQ, Zhang XH, et al. The oncometabolite 2-hydroxyglutarate inhibits microglial activation via the AMPK/mTOR/NF-kappaB pathway. Acta Pharm Sin. 2019;40:1292–302. https://doi.org/10.1038/s41401-019-0225-9.